

Direct Interaction of CASK/LIN-2 and Syndecan Heparan Sulfate Proteoglycan and Their Overlapping Distribution in Neuronal Synapses

Yi-Ping Hsueh,* Fu-Chia Yang,* Viktor Kharazia,[‡] Scott Naisbitt,* Alexandra R. Cohen,[§] Richard J. Weinberg,[‡] and Morgan Sheng*

*Howard Hughes Medical Institute and Department of Neurobiology, Massachusetts General Hospital and Harvard Medical School, Boston, Massachusetts 02114; [‡]Department of Cell Biology and Anatomy, University of North Carolina, Chapel Hill, North Carolina 27599; [§]Department of Cell Biology and Internal Medicine, Yale School of Medicine, New Haven, Connecticut 06520

Abstract. CASK, the rat homolog of a gene (*LIN-2*) required for vulval differentiation in *Caenorhabditis elegans*, is expressed in mammalian brain, but its function in neurons is unknown. CASK is distributed in a punctate somatodendritic pattern in neurons. By immunogold EM, CASK protein is concentrated in synapses, but is also present at nonsynaptic membranes and in intracellular compartments. This immunolocalization is consistent with biochemical studies showing the presence of CASK in soluble and synaptosomal membrane fractions and its enrichment in postsynaptic density fractions of rat brain. By yeast two-hybrid screening, a specific interaction was identified between the PDZ domain of CASK and the COOH terminal tail of syndecan-2, a cell surface heparan sulfate proteoglycan

(HSPG). The interaction was confirmed by coimmunoprecipitation from heterologous cells. In brain, syndecan-2 localizes specifically at synaptic junctions where it shows overlapping distribution with CASK, consistent with an interaction between these proteins in synapses. Cell surface HSPGs can bind to extracellular matrix proteins, and are required for the action of various heparin-binding polypeptide growth/differentiation factors. The synaptic localization of CASK and syndecan suggests a potential role for these proteins in adhesion and signaling at neuronal synapses.

Key words: CASK • LIN-2 • syndecan • heparan sulfate proteoglycan • PDZ domain

THE membrane-associated guanylate kinase homologs (MAGUKs)¹ are a large family of proteins typically localized at cell junctions. MAGUKs have a distinctive domain structure characterized by one or more NH₂-terminally located PDZ domains, a COOH-terminally located guanylate kinase-like (GK) domain, and an intervening SH3 domain (reviewed in Anderson, 1996; Kim, 1995; Sheng and Kim, 1996). All these domains appear to be important for mediating specific protein-protein interactions (Kim et al., 1997; Kornau et al., 1997; Sheng, 1996).

A role in the localization and clustering of synaptic ion

channels and receptors has been proposed for the PSD-95 family of MAGUKs, which appear to be important for molecular organization of the postsynaptic membrane in neurons (reviewed in Kornau et al., 1997; Sheng, 1996). The interactions between ion channels and PSD-95 are mediated by the PDZ domains of the MAGUK protein binding directly to the cytoplasmic COOH-terminal tails of the channel proteins. In addition to membrane ion channels and receptors, PSD-95 family proteins also interact with intracellular proteins involved in signaling or associated with the cytoskeleton, such as APC (Matsumine et al., 1996), GKAP (Kim et al., 1997; Naisbitt et al., 1997; Satoh et al., 1997; Takeuchi et al., 1997), protein 4.1 (Lue et al., 1996; Marfatia et al., 1996), and neuronal nitric oxide synthase (Brenman et al., 1996). Furthermore, members of the PSD-95 family of MAGUKs can form homo- or heteromultimers with themselves, resulting in aggregation of their binding partners (Hsueh et al., 1997; Kim et al., 1996; Kim et al., 1997; Kim et al., 1995). A general picture now emerging is that MAGUKs function as multidomain scaffold proteins that organize specific signaling complexes at defined membrane locations.

Address all correspondence to Morgan Sheng, Howard Hughes Medical Institute, Massachusetts General Hospital (Wel 423), 50 Blossom Street, Boston, MA 02114. Tel.: 617-724-2800; FAX: 617-724-2805; E-mail: sheng@helix.mgh.harvard.edu

1. *Abbreviations used in this paper:* aa, amino acid; ECM, extracellular matrix; EGFR, EGF receptor; HCASK, rabbit anti-human CASK; HSPG, heparan sulfate proteoglycan; Kv1.4-EFYA, Kv1.4-syndecan-2 chimeric protein; MAGUK, membrane associated guanylate kinase; MB, maleate buffer; PB, phosphate buffer; PSD, postsynaptic density; SYN-2C, syndecan-2 antibody.

LIN-2 is a member of the MAGUK superfamily that contains an NH₂-terminal calmodulin-dependent kinase (CaMK)-like domain preceding its single PDZ domain, SH3 domain, and GK domain (Hoskins et al., 1996). In *C. elegans*, LIN-2 is required for vulval differentiation, and may be involved in the proper localization of LET-23, an EGF receptor (EGFR) homolog important in the vulval differentiation pathway (Hoskins et al., 1996; Simske et al., 1996). LIN-2 is thus genetically implicated in receptor tyrosine kinase signaling. However, it is not LIN-2 itself, but another PDZ-containing protein, LIN-7, that binds directly to the intracellular COOH terminus of LET23/EGFR (Simske et al., 1996). Hence, the biochemical and cell biological functions of LIN-2 remain unclear. In particular, the physiological binding partner(s) for the PDZ domain of LIN-2 are unknown.

LIN-2 homologs have been identified in *Drosophila* and in mammals (Dimitratos et al., 1997; Hata et al., 1996). CASK, a rat homolog of LIN-2, was isolated via its ability to bind in the yeast two-hybrid system to the neuroligins, a family of neuronal cell surface proteins (Hata et al., 1996). Here we show that via its PDZ domain, CASK/LIN-2 can bind directly to the COOH-terminal tail of the syndecans, a family of transmembrane heparan sulfate proteoglycans (HSPGs). We also report the subcellular distribution of CASK and syndecan-2 in neurons of rat brain at both light microscopy (LM) and EM levels, and present evidence for an *in vivo* interaction between CASK and syndecan in neuronal synapses.

Materials and Methods

Antibodies

CASK (CASK-FYG) antibodies and syndecan-2 (Syn-2C) antibodies were raised in rabbits against the synthetic peptide CFYGDPEELPDFSED, corresponding to amino acids 320–334 of CASK, and the synthetic peptide RKKDEGSYDLGERKPSC, corresponding to amino acids 182–197 of rat syndecan-2, respectively. The terminal cysteine residues were added for coupling purposes. Both antibodies were affinity-purified using their respective immunogen peptide coupled to a Sulfolink column (Pierce Chemical Co., Rockford, IL). Rabbit anti-human CASK (hCASK) antiserum is described in Cohen et al. (cosubmitted manuscript). Anti-SAP97 and anti-PSD95 CSK antibodies were described in Kim et al. (1996). Anti-Myc mouse monoclonal antibody (9E10) was purchased from Santa Cruz Biotechnology (Santa Cruz, CA). MSE-2 antiserum, a gift from Dr. Merton Bernfield, was raised against the nonconserved extracellular region of syndecan-2, and has been described (Kim et al., 1994).

Plasmid Constructs

Rat syndecan-2 cDNA was generously provided by Dr. Graham Cowling (Manchester University, United Kingdom). The coding region of rat syndecan-2 was PCR-amplified and subcloned into the KpnI and EcoRI site of mammalian expression vector GW1-CMV. Two oligonucleotides, one containing an XbaI site, the myc epitope (EQKLISEEDL), and the sequence GACCTTGAGAACGCAAACCG (corresponding to aa 190–196 of syndecan-2), and the other containing an XbaI site and the sequence GTAGCTTCTTCGTCTTTC TT (corresponding to aa 183–189 of rat syndecan-2), were applied in reverse PCR for construction of myc-tagged syndecan-2. The amplified product was digested with XbaI and then religated. The Kv1.4-syndecan-2 chimeric protein (Kv1.4-EFYA) was constructed by PCR using Kv1.4 cDNA as template and a 3' end primer encoding the last four amino acids (aa) of syndecan-2 and aa 648–651 of Kv1.4.

CASK cDNA was amplified by reverse transcription PCR from rat brain first-strand cDNA library, and was subcloned into pGW1-CMV. In addition, we obtained CASK cDNA as a gift from Dr. Thomas C. Südhof.

For myc-tagged CASK construction, an AscI site was created between aa 599 and 560 of CASK by inverse PCR. A double-stranded oligonucleotide encoding the myc epitope was inserted into the AscI site.

Transfection, Immunoprecipitation, Biochemical Fractionation, and Immunoblotting

COS-7 cells in 35-mm plates at 50–70% confluency were incubated with a 1-ml OPTI-MEM (GIBCO BRL, Gaithersburg, MD) mixture containing 1.6 µg DNA and 6 µl Lipofectamine (GIBCO-BRL) for 5 h followed by incubation in DMEM medium. 48 h later, cells were harvested and lysed in RIPA buffer. Immunoprecipitation from RIPA cell lysates has been described (Hsueh et al., 1997), except that Myc antibody 9E10-conjugated agarose (Santa Cruz Biotechnology) was used to precipitate myc-tagged proteins directly. Fractionation of brain membranes and PSDs was performed as described by Cho et al. (1992). Immunoblotting with enhanced chemiluminescence reagents was performed as described (Sheng et al., 1993). hCASK antiserum was used at a 1:2,000 dilution; affinity-purified primary antibodies were used at 2 µg/ml (Syn-2C antibody), 0.5 µg/ml (CASK-FYG antibody), 0.2 µg/ml (PSD-95 CSK antibody), 1 µg/ml (SAP97 antibody), or 0.2 µg/ml (anti-Myc antibody 9E10).

Immunohistochemistry

Immunohistochemistry was performed on Vibratome-cut (Ted Pella, Inc., Redding, CA) 50-µm floating brain sections from rats (~6 wk old; Harlan Sprague Dawley Inc., Indianapolis, IN) perfused transcardially with 4% paraformaldehyde and permeabilized with either 0.1% Triton X-100 or 50% ethanol. Rat brain sections were incubated with affinity-purified primary antibodies at 2 µg/ml at room temperature overnight. For DAB staining, Vectastain Elite ABC kit (Vector Labs, Inc., Burlingame, CA) was used as described (Sheng et al., 1994). For immunofluorescent staining, Cy3- or FITC-conjugated secondary antibodies (Jackson ImmunoResearch Laboratories, Inc., West Grove, PA) were used at the dilution of 1:1,000 and 1:200, respectively.

Double-label immunofluorescence with two antibodies raised from the same species (rabbit) was performed as described in Shindler and Roth (1996) with some modifications. The brain sections were incubated with a very low concentration (0.05 µg/ml) of Syn-2C antibodies in PBS with 0.5% blocking reagent (TSA direct kit; Dupont-NEN, Boston, MA) at room temperature overnight. After washing three times with PBST (1× PBS with 0.05% Tween-20), the sections were incubated with biotinylated anti-rabbit antibody (Jackson ImmunoResearch Laboratories, Inc.) at 1:1,000 at room temperature for 2 h, and were incubated with streptavidin-conjugated horseradish peroxidase (TSA direct kit; Dupont-NEN) at 1:100 for a further 30–60 min. Finally, FITC-conjugated tyramide (TSA direct kit; Dupont-NEN) was applied at 1:50 in amplification diluent (TSA direct kit; Dupont-NEN) for 5–10 min. After washing three times with PBST, these rat brain sections were then processed for conventional immunofluorescent CASK staining using Cy-3-conjugated secondary antibodies as described above. At the low concentrations of Syn-2C antibodies used, no Syn-2C signal could be detected with Cy3-conjugated anti-rabbit secondary antibodies. Results were viewed with an Axioskop microscope (Carl Zeiss Inc., Thornwood, NY) or a confocal microscope (MRC-1000; Bio-Rad Laboratories, Hercules, CA), and digitized images were processed for publication using Adobe Photoshop.

Electron Microscopy

For electron microscopy, pentobarbital-anesthetized (60 mg/kg) male Sprague-Dawley rats (250–350 g) were perfused intraaortically with mixed aldehyde fixatives (0.2% glutaraldehyde and 4% depolymerized paraformaldehyde for immunoperoxidase staining; 2% glutaraldehyde and 2% paraformaldehyde for immunogold) in phosphate buffer (PB), pH 7.4, after a brief flush with heparinized saline. The brain was removed and immersed in the same fixative for 2 h; 40-µm sections were cut on a Vibratome and collected in PB. For immunogold, sections were embedded directly into resin (see below). For preembedding immunoperoxidase staining, floating sections in glass vials were treated for 30 min in 1% sodium borohydride in PB, permeabilized for 30 min with 50% EtOH, and then incubated for 10 min in 3% hydrogen peroxide, blocked in 10% donkey serum, and incubated in primary antibody (diluted 1:100–1:1,000) on a shaker overnight. Sections were then rinsed, incubated in secondary antibody (biotinylated, donkey anti-rabbit; Jackson ImmunoResearch Laboratories, Inc., 1:200) for 2 h, rinsed, incubated in ExtrAvidin (1:5,000;

Sigma Chemical Co., St. Louis, MO) for 2 h, rinsed, and reacted with diaminobenzidine to visualize antibody-binding sites. Sections were then poststained 1 h in 1% platinum chloride in maleate buffer (MB) and infiltrated with resin.

Embedding was performed according to modifications of an osmium-free protocol (Phend et al., 1995). In brief, sections were incubated over ice in 0.1% filipin/0.1% digitonin (Sigma Chemical Co.) in MB for 20 min, for 40 min with 1% tannic acid in MB, for 20 min in 0.1% CaCl_2 , for 40 min in 1% uranyl acetate, and then for 20 min in 0.5% IrBr_4 (Pfaltz and Bauer, Inc., Waterbury, CT). Sections were dehydrated through graded alcohols and propylene oxide, and then infiltrated with Epon-Spurr resin (Electron Microscopy Sciences, Fort Washington, PA). Wafers prepared with ACLAR plastic (Pelco; Ted Pella, Inc.) were polymerized at 60°C for 24–36 h. Small chips of the polymerized wafers were glued to plastic blocks; and thin sections cut with a diamond knife were collected on copper mesh grids, poststained with uranyl acetate and lead citrate, and examined with a CX200 microscope (JEOL USA, Inc., Peabody, MA). For immunogold staining, sections were collected on nickel mesh grids and processed according to methods described in Phend et al. (1992). Primary antibody concentrations were 1:100–1:400; the secondary was donkey anti-rabbit serum, conjugated to 18-nm gold particles (Jackson ImmunoResearch Laboratories, Inc.). After immunoprocessing, grids were briefly immersed in 1% glutaraldehyde, rinsed, and poststained as described above.

Yeast Two-hybrid Screen and Analysis of CASK-Syndecan-2 Interaction

Two-hybrid screening was done using the L40 yeast strain harboring reporter genes HIS3 and LacZ under the control of upstream LexA-binding sites, as described previously (Kim et al., 1995). The PDZ domain of hCASK (which is identical at the aa level with rat CASK) was subcloned into pBHA (LexA fusion vector), and was used to screen rat and human brain cDNA libraries constructed in pGAD10 (GAL4 activation domain vector; CLONTECH Laboratories, Inc., Palo Alto, CA). COOH-terminal deletion mutants of syndecan-2 were created by PCR and subcloned into pGAD10 to generate GAL-4 activation domain fusions. The interactions of CASK and syndecan were tested in yeast two-hybrid assays by using HIS3 and LacZ as reporter genes (Kim et al., 1995).

Results

Subcellular Fractionation of CASK in Rat Brain

To study CASK expression in rat brain at the protein level, we raised antibodies (termed CASK-FYG) against a peptide sequence located between the CaMK and PDZ domains of CASK. The specificity of these anti-CASK antibodies was examined by Western blotting of transfected heterologous cells and brain. CASK-FYG antibodies recognized a dominant band of ~110 kD in extracts of COS-7 cells transfected with CASK cDNA, but not with vector alone (Fig. 1A). In rat brain, CASK was detected as an ~110-kD protein that is mainly associated with membranes, though a significant fraction was also present in soluble fractions (Fig. 1B). By immunoblotting, CASK is broadly expressed in several brain regions, including neocortex, cerebellum, hippocampus, and brain stem. The same ~110-kD band in brain and in CASK-transfected COS cells was recognized by an independent antiserum raised against an hCASK fusion protein (Fig. 1B and data not shown).

The membrane-associated CASK further purified into the postsynaptic density (PSD) fraction, in which it was resistant to extraction by Triton X-100 (PSD I and PSD II) and by Triton X-100 and sarkosyl (PSD III; Fig. 1C). The degree of CASK enrichment in the PSD fractions, however, was weaker than that seen with PSD-95, a standard marker for PSDs (Fig. 1C). Nevertheless, enrichment of CASK in purified PSDs showed specificity, since SAP97,

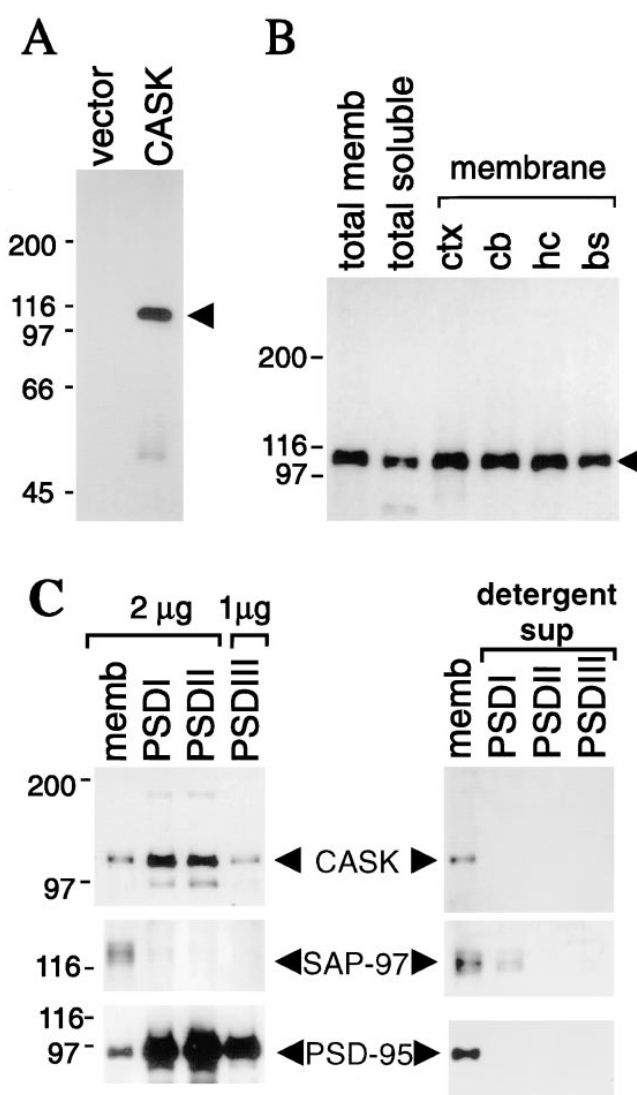


Figure 1. Regional distribution and subcellular fractionation of CASK in adult rat brain. (A) Specificity of CASK-FYG peptide antibody. Lysates of COS-7 cells transfected with CASK cDNA or vector alone were immunoblotted with affinity-purified CASK-FYG antibodies. Arrowhead points to specific CASK band of ~110 kD. (B) Membrane association and regional expression of CASK. Whole-brain synaptosomal membrane and soluble fractions, and synaptosomal membranes from different regions of adult rat brain, were immunoblotted for CASK using anti-hCASK antiserum. Lanes were loaded as follows (10 μg protein per lane): total memb, lysed crude synaptosomal membrane fraction of whole brain; total soluble, S100 supernatant fraction of whole brain; and lysed synaptosomal membranes from neocortex (ctx), cerebellum (cb), hippocampus (hp), and brain stem (bs). Identical results were obtained with CASK-FYG antibodies (not shown). (C) Enrichment and detergent extractability of CASK in PSD fractions, compared with PSD-95 and SAP97. Lanes were loaded as follows: memb, lysed crude synaptosomal membrane fraction from whole brain; purified PSD fractions extracted with Triton X-100 once (PSD I), twice (PSD II), or with Triton X-100 followed by sarkosyl (PSD III). Amounts of protein loaded in each lane are indicated. Detergent supernatants of each PSD fraction (2 μg protein) were also immunoblotted. Positions of molecular size standards are shown in kD.

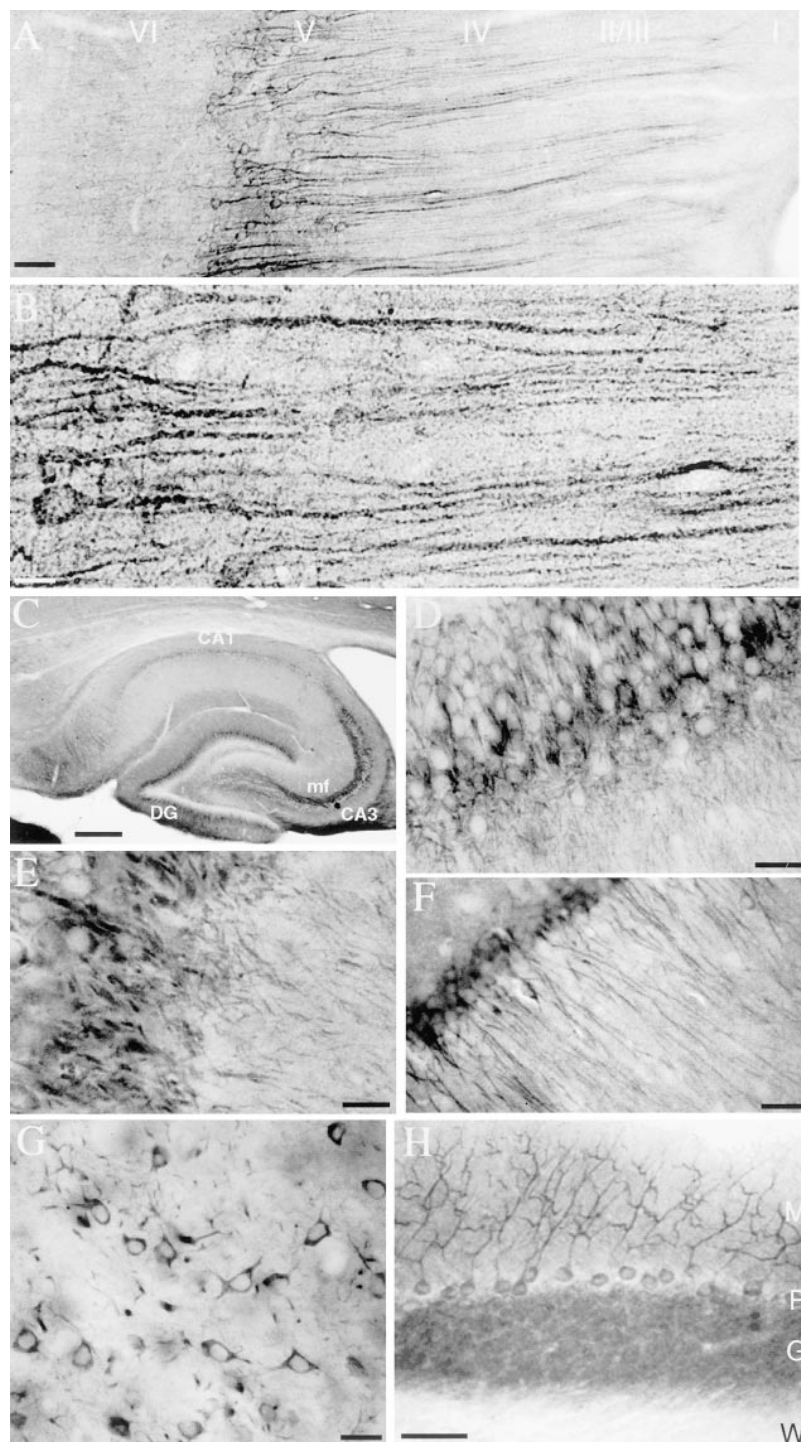


Figure 2. DAB immunohistochemistry of CASK in adult rat brain. (A) Layer-specific staining in neocortex; (B) heavily stained cortical layer 5 pyramidal neurons and their apical dendrites; (C) hippocampal formation showing staining of dendritic fields in all regions and of mossy fiber tract. Neurons show CASK immunoreactivity in a somatodendritic pattern; examples shown here are: (D) granule cells of dentate gyrus; (E) pyramidal neurons of CA3; (F) pyramidal neurons of CA1; (G) neurons in the thalamus; and (H) Purkinje cells of cerebellum. Staining was abolished by preincubating CASK-FYG antibodies with excess immunogen peptide (not shown). DG, dentate gyrus; mf, mossy fiber tract; M, molecular layer; P, Purkinje cell layer; G, granule cell layer; W, white matter. Bars: (A) 100 μ m; (B) 20 μ m; (C) 650 μ m; (D–F) 30 μ m; (G), 60 μ m; and (H) 200 μ m.

an axonal and presynaptic protein (Müller et al., 1995), was depleted in PSDs. These biochemical fractionation studies suggest that CASK is present in the PSD, but that it is not as selectively concentrated in synapses as is PSD-95. This interpretation is supported by immunocytochemical studies (see below).

Immunohistochemical Distribution of CASK in Rat Brain

Affinity-purified CASK-FYG antibodies and anti-hCASK

antibodies were used to localize CASK in sections from rat brain. As with Western blotting, these two independent antibodies gave specific staining patterns that were strikingly similar to each other (data not shown), providing strong support that they reveal the true distribution of CASK protein. CASK protein is expressed widely in the brain, and is distributed in a somatodendritic pattern, predominantly in neurons (Fig. 2). In cerebral cortex, pyramidal cells showed strong immunoreactivity in cell bodies and in apical dendrites; nuclei appeared unstained. The apical dendritic staining extended from the proximal trunk

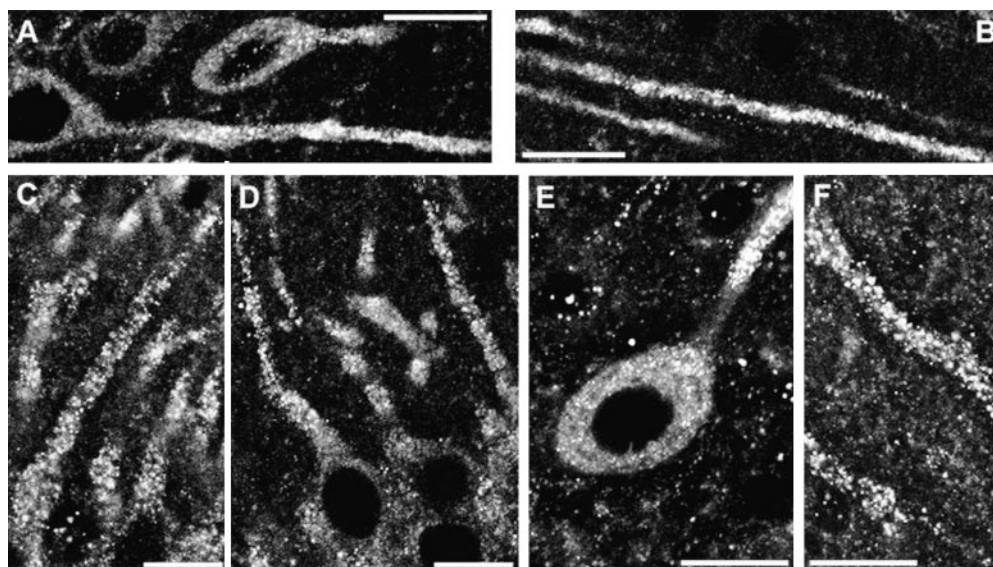


Figure 3. Localization of CASK in rat brain neurons by immunofluorescence confocal microscopy. Punctate CASK immunoreactivity is seen on top of diffuse intracellular staining in neuronal somata and dendrites. (A) Layer 5 pyramidal cells of cerebral cortex; (B) apical dendrites of layer 5 pyramidal cells; (C and D) CA1 pyramidal neurons; (E and F) cell body and dendrites of Purkinje cells in the cerebellum. A similar staining pattern was seen with anti-hCASK antiserum (not shown). Bars: (A and B) 50 μ m; (C and D), 10 μ m; (E and F), 30 μ m.

to the terminal branches, and was most prominent for layer 5 pyramidal neurons (Fig. 2, *A* and *B*). Layer 2/3 pyramidal neurons were also stained, though at lower intensity, and layer 4 cells were relatively spared of labeling. The punctate nature of CASK staining seen on pyramidal cell dendrites is consistent with a synaptic localization (Fig. 2 *B*), though there was also substantial intracellular immunoreactivity in somata and proximal dendrites.

In the hippocampal formation, CASK protein was present in dentate granule cells and in CA1 and CA3 pyramidal cells in a somatodendritic distribution (Fig. 2, *C–F*). In addition, however, staining was noted in the mossy fiber tract (Fig. 2 *C*) where axons from the dentate gyrus granule cells run adjacent to the cell bodies of CA3 pyramidal neurons. CASK immunoreactivity was also prominent in neurons of the thalamus, especially in somata and proximal dendrites (Fig. 2 *G*). In the cerebellum, the cell bodies and dendrites of Purkinje cells were intensely labeled, and the granule cell layer showed moderate staining (Fig. 2 *H*). In both forebrain and hindbrain, the neuropil showed significant CASK staining, whereas white matter tracts were relatively spared.

Higher resolution immunofluorescence confocal microscopy with CASK-FYG antibodies revealed punctate staining on top of a relatively diffuse staining in intracellular compartments and in major dendrites (Fig. 3). Punctate labeling was most prominent along dendritic processes, suggesting a possible synaptic localization of CASK. This subcellular distribution pattern is exemplified in pyramidal neurons of cortex and hippocampus (Fig. 3, *A–D*). In cerebellum, CASK antibodies also revealed punctate staining in somata and along major dendrites of Purkinje cells (Fig. 3, *E* and *F*).

Ultrastructural localization of CASK was obtained by postembedding immunogold EM. The highest density of CASK labeling was found at asymmetric (presumed excitatory) synapses (Fig. 4, *A*, *B*, *E*, and *F*), but was also seen at symmetric (presumed inhibitory) synapses (Fig. 4, *B*, *C*, and *D*). Quantitative analysis of immunogold distribution showed that the peak of CASK labeling was closely associated with the synaptic membranes, and was roughly sym-

metrically disposed across the synaptic cleft (see Fig. 8, *left*), implying the presence of CASK in both presynaptic and postsynaptic compartments close to the membrane. In addition to its association with synaptic membranes and adjacent cytoplasm, CASK was also present at a lower density at nonsynaptic membranes (Fig. 4, *B*, *C*, and *F*; see Fig. 8, *right*). Cytoplasmic CASK labeling was observed in somata and in dendritic shafts, where it appeared to be often associated with polyribosomes (Fig. 4 *B*). The presence of CASK in intracellular compartments is also reflected in the particle density plot (Fig. 8, *left*), which shows a broad major peak with smaller peaks of immunogold density some distance (~ 100 nm) from the synaptic membranes. These ultrastructural findings correlate well with the localization of CASK at the LM level.

In summary, CASK is distributed in a somatodendritic pattern in neurons, and is enriched but not exclusively localized in synapses. CASK is also present at nonsynaptic plasma membranes and in intracellular compartments. These immunocytochemical findings are consistent with the biochemical fractionation profile of CASK, which shows incomplete membrane association (Fig. 1 *B*) and only a moderate enrichment in PSD fractions (Fig. 1 *C*).

The CASK PDZ Domain Binds to the COOH Terminus of Syndecan

The COOH terminal tail of neurexin has been shown to interact with CASK (Hata et al., 1996), possibly via CASK's PDZ domain. Since PDZ domains in general can bind to multiple partners with compatible COOH-terminal sequences (Kornau et al., 1997; Sheng, 1996; Sheng and Kim, 1996; Songyang et al., 1997) as well as to heterologous PDZ domains (Brennan et al., 1996), we sought to identify other potential ligands for CASK. Using the single PDZ domain of CASK as bait in a yeast two-hybrid screen, three interacting cDNA clones were isolated from brain cDNA libraries (Table I). The most strongly interacting cDNA encoded the COOH-terminal region of a known protein, the transmembrane HSPG syndecan-2 (which terminates in the sequence -EFYA). The remain-

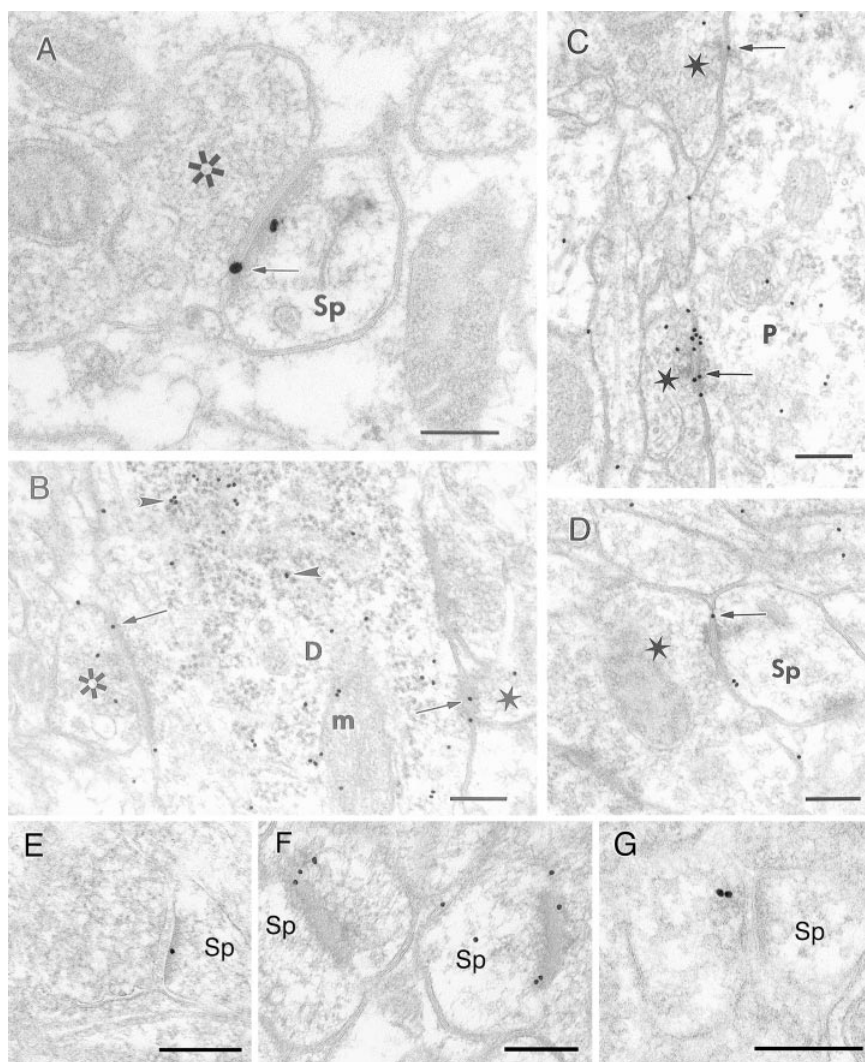


Figure 4. Subcellular localization of CASK by immunogold EM. (A) Electron micrograph of an asymmetric axospinous synapse shows CASK labeling over synaptic membrane and postsynaptic density (silver-intensified 1-nm gold particles used to optimize accuracy of localization). (B) Dendritic shaft immunopositive for CASK. Labeling (18-nm gold particles) is present over polyribosomes (arrow-heads). Two synapses on this dendrite, one of asymmetric type (asterisk, left), and another of symmetric type (star, right) are also labeled (arrows). CASK is also seen at nonsynaptic plasma membranes. (C) CASK-positive neuronal perikaryon (P) contacted by two axon terminal-making symmetric synapses (likely to use GABA as transmitter); both synapses are immunopositive for CASK (arrows). (D) Labeling associated with synaptic membranes adjacent to the active zone of the axospinous synapse. (E) Labeling over PSD of asymmetric axospinous synapse. (F) CASK labeling concentrated over two obliquely sectioned axospinous synapses. An additional gold particle is visible in the spine cytoplasm; another nearby particle is associated with the nonsynaptic plasma membrane. (G) Presynaptic labeling at axospinous synapses. Asterisks mark axon terminals making asymmetric synaptic contacts; stars mark terminals making symmetric contacts. D, dendrite; m, mitochondrion; P, perikaryon; Sp, spine. Bars, 200 nm.

ing two cDNAs encoded the COOH-terminal regions of two proteins of unknown function and with no homology to other sequences in the database, one terminating in -EFQV, and the other ending in -YFDV. Conservation of the COOH-terminal sequence of the interacting clones suggests that this region is involved in binding to the PDZ domain of CASK. This result was confirmed by deletion of the last three residues of syndecan-2, which abolished its interaction with CASK's PDZ in the two-hybrid system (Table I). In the course of this analysis, we also confirmed that the COOH terminus of neuexin can bind to the CASK PDZ domain.

To confirm that full-length CASK and syndecan-2 proteins can associate with each other, we performed coimmunoprecipitation assays in heterologous cells. From COS cells cotransfected with CASK and myc-tagged syndecan-2, myc antibodies were able to precipitate CASK in addition to myc-tagged syndecan-2 (Fig. 5 A). CASK expressed by itself, however, was not immunoprecipitated by myc antibodies. These data indicate that full-length syndecan-2 and full-length CASK can form a complex in a mammalian cell environment.

The results of yeast two-hybrid assays (Table I) indicated that the COOH terminus of syndecan-2 is necessary

for binding to the CASK PDZ domain. To test whether the COOH-terminal residues are sufficient for this interaction, we constructed a Kv1.4-EFYA in which the last four amino acids of the K⁺ channel Kv1.4 (-ETDV) are replaced by the corresponding syndecan-2 COOH terminus (-EFYA). In heterologous cells, this Kv1.4-EFYA chimeric protein could be coprecipitated with myc-tagged CASK by CASK-FYG antibodies (Fig. 5 B). In contrast, wild-type Kv1.4 was not coprecipitated with CASK (Fig. 5 B), although it could be efficiently coimmunoprecipitated with PSD-95 (Kim et al., 1996). These results indicate that the COOH-terminal four amino acids of syndecan-2 (EFYA) are sufficient to confer CASK PDZ-binding on a heterologous membrane protein. Since all four known members of the syndecan family terminate with the identical sequence EFYA (Bernfield et al., 1992; Carey, 1997), this finding implies that all four syndecans can bind to the PDZ domain of CASK.

Synaptic Localization of Syndecan-2

To investigate the putative interaction of syndecan HSPGs and CASK in vivo, we used Syn-2C to localize syndecan-2 in rat brain. At high resolution, the Syn-2C immunostain-

Table 1. Analysis of CASK PDZ Domain Interactions by Yeast Two-Hybrid System

	COOH-terminus	CASK/PDZ	
		β -gal	His
Clone 1 (Syndecan-2)	KEFYA	+++	+
Clone 2 (G2)	FEFQV	++	+
Clone 3	TYFDV	+	+
Syn-2 wild-type	KEFYA	+++	+
Syn-2 Δ FYA	KE---	-	-
Neurexin	KEYYV	+++	+

Clones 1, 2, and 3 were isolated by a yeast two-hybrid screen of brain cDNA libraries using the CASK PDZ domain as bait. Their COOH terminal sequences (last five amino acids) are shown in single letter code. Clone 1 is a COOH-terminal fragment of syndecan-2 (aa 72–aa 201). Clone 2 is a COOH-terminal fragment of a gene deposited in the databases as sequence G2, accession no. U10991. Clone 3 is a novel cDNA sequence. The COOH-terminal sequence of syndecan-2 is compared with neurexin. Deletion of the last three residues of syndecan-2 (Syn2 Δ FYA) abolishes its binding to the CASK PDZ domain. Yeast two-hybrid interactions are semiquantified based on induction of reporter genes β -galactosidase and HIS3. HIS3 activity was measured by the percentage of colonies growing on histidine-lacking medium: +++, >60%; ++, 30–60%; +, 10–30%; –, no significant growth. β -galactosidase activity was measured by the time taken for colonies to turn blue in X-gal filter lift assay at room temperature: +++, <45 min; ++, 45–90 min; +, 90–240 min; –, no significant activity. By immunoblotting, expression of the syndecan-2 Δ FYA construct in yeast was similar to that of wild-type syndecan-2 (data not shown).

ing pattern in all regions of the brain was notably punctate and suggestive of synaptic labeling (Fig. 6). The specific concentration of Syn-2C immunoreactivity in synapses was revealed by its colocalization with the synaptic vesicle marker synaptophysin in double-labeling studies (Fig. 6). Examples of punctate colocalization of Syn-2C and synaptophysin staining are shown from the stratum lucidum of the hippocampus (Fig. 6A), the neuropil of the cerebral cortex (Fig. 6B), the glomeruli of the granule cell layer of the cerebellum (Fig. 6C), and the glomeruli of the olfactory bulb

(Fig. 6D). In all areas of the brain, cell bodies and major dendrites were relatively spared of Syn-2C labeling (Fig. 6).

To confirm the specificity of Syn-2C staining, we performed immunocytochemistry with a second independent antiserum raised against the extracellular region of syndecan-2. This antibody (MSE-2; Kim et al., 1994) gave a synaptic pattern of staining similar to that of Syn-2C, including the glomeruli of the cerebellar granular layer (Fig. 6E). The similar staining pattern with two independent antibodies to syndecan-2 provides strong evidence that syndecan-2 is specifically localized in neuronal synapses.

Localization of Syndecan in Synapses by Immunogold EM

To verify the synaptic localization of syndecan-2 at ultrastructural resolution, we performed EM immunocytochemistry. Type 1 (asymmetric) synapses were specifically labeled by Syn-2C antibodies as revealed by preembedding immunoperoxidase staining (Fig. 7A). Electron-dense reaction product was prominent at the PSD as well as in the presynaptic axon terminal. Labeling was observed close to the synaptic membrane, and in many cases could also be seen some distance from the synapse, particularly on the presynaptic side. Postembedding immunogold staining confirmed a heavy concentration of Syn-2C immunoreactivity, specifically at asymmetric synapses. By far the highest density labeling was closely associated with the synaptic membranes, but in addition a lower density of particles was detected over the presynaptic axon terminal some distance from the synapse (Fig. 7, B–D, F, and G; see quantitation in Fig. 8). Outside of asymmetric synapses, Syn-2C labeling was present sparsely at nonsynaptic sites of membrane–membrane apposition,

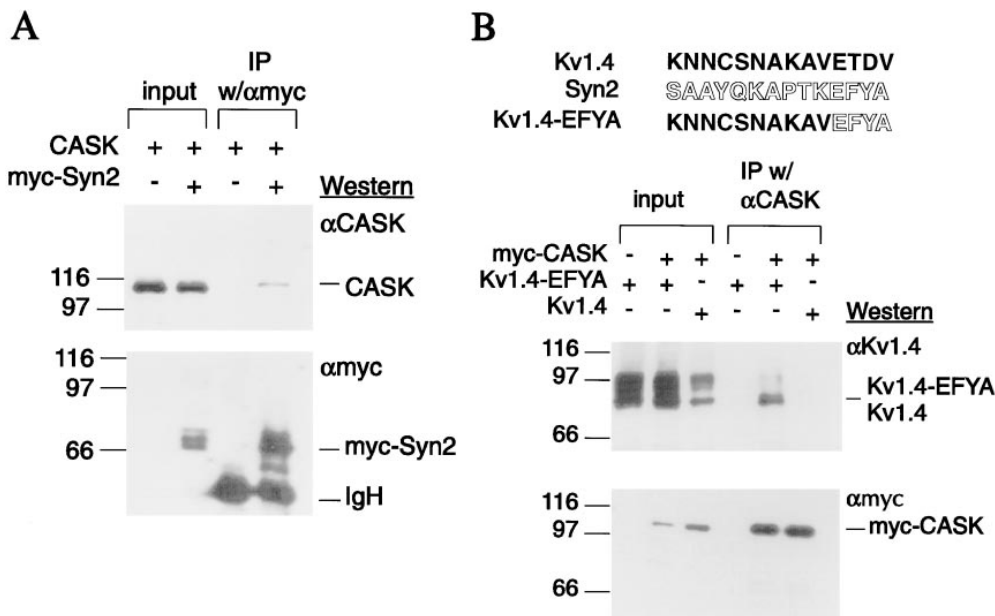


Figure 5. COOH-terminal- Δ FYA motif of syndecan-2 is sufficient to mediate association with CASK. (A) Coimmunoprecipitation of CASK and syndecan-2. COS-7 cells were transfected with CASK and/or myc-tagged syndecan-2 as indicated, and were then lysed and immunoprecipitated with anti-myc antibodies. Immunoprecipitates were Western-blotted for CASK and myc-syndecan-2. CASK was precipitated by anti-myc antibody only when CASK was coexpressed with myc-syndecan-2. (B) The COOH-terminal four aas of syndecan-2 are sufficient for association with CASK. The COOH-terminal sequences of Shaker channel subunit Kv1.4 and syndecan-2 are aligned at the

top. Kv1.4-EFYA chimeric construct contains full-length Kv1.4 except that the last four aas were substituted with the corresponding syndecan-2 COOH terminus. COS-7 cells were transfected with various combinations of myc-tagged CASK, Kv1.4-EFYA, and wild-type Kv1.4, as indicated. Immunoprecipitations were performed with CASK-FYG antibodies, and the precipitates were immunoblotted sequentially with anti-Kv1.4 and anti-myc antibodies, as indicated. Kv1.4-EFYA, but not wild-type Kv1.4, could be coprecipitated with CASK. Input lanes were loaded with 10% of the lysate used for the immunoprecipitation reactions.

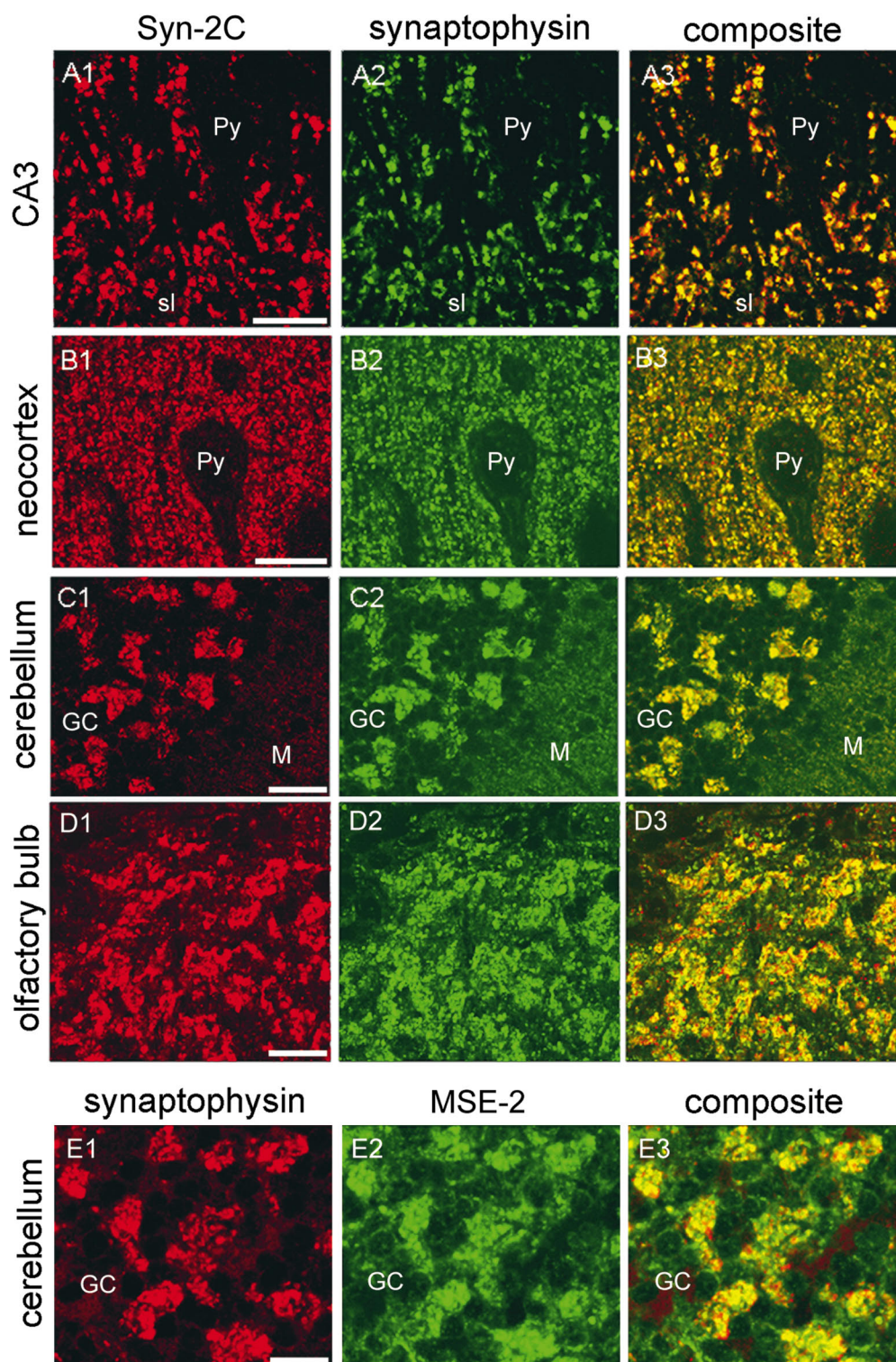


Figure 6. Synaptic localization of syndecan-2 in rat brain, revealed by colocalization of Syn-2C and synaptophysin staining. Double-label confocal imaging of Syn-2C and synaptophysin staining in (A) CA3; (B) neocortex; (C) cerebellum; and (D) olfactory bulb. (E) The granule cell layer of cerebellum is double-labeled with synaptophysin antibody and MSE-2, an independent antiserum that specifically recognizes the extracellular domain of syndecan-2. Each group of images ([A1–A3], [B1–B3], [C1–C3], [D1–D3]) represents the same field visualized for Syn-2C (Cy3/red) or for synaptophysin (FITC/green), as indicated. (E) Syndecan-2 (MSE-2) was viewed with FITC/green and synaptophysin with Cy3/red. Composite images (A3–E3) show colocalization of syndecan and synaptophysin in yellow. GC, granule cell layer; M, molecular layer; Py, pyramidal cell bodies; sl, stratum lucidum. Bars: (A–D) 20 μ m; (E) 10 μ m.

and only occasionally within the cytoplasm of dendritic shafts (Fig. 7, D and E). In short, these LM and EM studies indicate that syndecan-2 is highly concentrated at asymmetric (presumably excitatory) synapses of rat brain, apparently on both pre- and postsynaptic sides of the synapse.

Colocalization of CASK and Syndecan-2 In Vivo

Based on subcellular localization of the individual pro-

teins, we reasoned that CASK and syndecan-2 distribution might overlap in brain synapses. This prediction was confirmed by colocalization of these two proteins in rat brain by double-label confocal microscopy (Fig. 9). An example of syndecan-2 colocalization with CASK is in the mossy fiber tract of the hippocampus (Fig. 9 A). Partial colocalization (i.e., overlap) was also seen in a punctate pattern along the dendrites of hippocampal pyramidal neurons (Fig. 9, B and C). The partial overlap occurs because Syn-

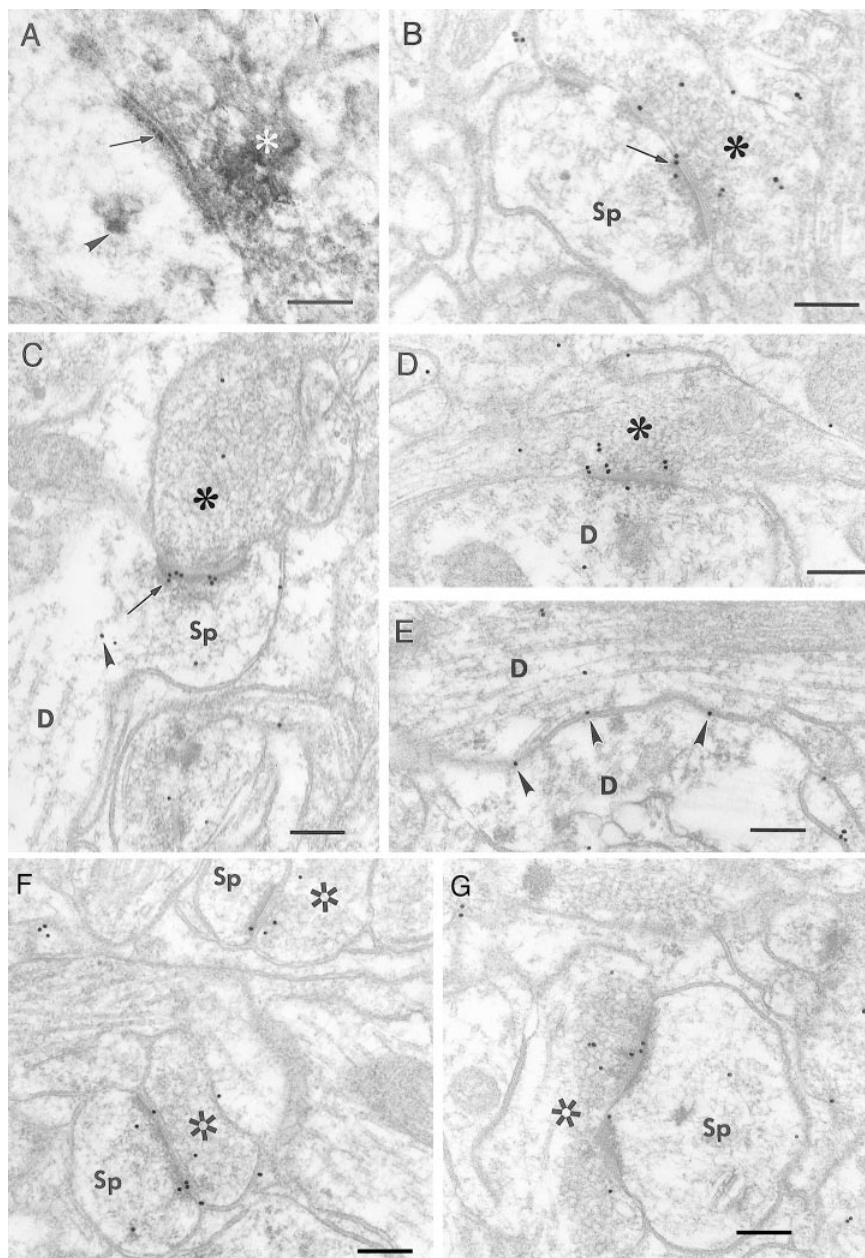


Figure 7. EM localization of syndecan-2. (A) Type 1 (asymmetric) synapse immunopositive for Syn-2C, as revealed by preembedding immunoperoxidase staining. Electron-dense reaction product is prominent in the presynaptic axon terminal (white asterisk). It is also in the adjacent dendrite, both at the postsynaptic density (arrow) and at some distance from the synapse (arrowhead). (B) Postembedding immunogold staining (18-nm particles). Arrow points to an immunopositive asymmetric synapse; labeling can be seen at the synaptic membrane. Labeling is also seen at lower density over the presynaptic axon terminal. (C) Arrow points to an immunopositive axospinous synapse. Dense labeling at the synaptic membrane (arrow) contrasts with weaker labeling over the axon terminal. Arrowhead points to labeling at the base of the dendritic spine. (D) Immunopositive asymmetric axodendritic synapse. In this example labeling is more conspicuous in presynaptic axon terminal than in postsynaptic dendritic shaft. (E) Labeling at nonsynaptic dendrodendritic apposition. Such nonsynaptic labeling, though always sparse, was strongest at the plasma membrane (arrowheads). Occasional labeling is also seen within dendrites. (F) Field showing two immunopositive axospinous synapses. Gold particles concentrate around synaptic active zones. (G) Perforated axospinous synapse showing concentration of syndecan-2 labeling at the synaptic membranes and in the axoplasm of the presynaptic terminal. Asterisks mark presynaptic terminals. D, dendritic profile; Sp, spine. Bars, 200 nm.

2C immunoreactivity is specifically localized to synaptic puncta, whereas CASK shows additional extensive staining in somata and major dendrites. Distinctive subcellular distributions of CASK and syndecan with overlapping localization in neuronal synapses is also shown graphically by quantitative comparison of their immunogold distributions (Fig. 8).

We tried to demonstrate biochemical association of CASK and syndecan-2 in brain, but failed to obtain convincing coimmunoprecipitation of these two proteins from detergent extracts of synaptosomal membranes. Several reasons may account for this inability: first, membrane-bound CASK is relatively insoluble and requires harsh detergents for extraction that may lead to disruption of the complex; second, our syndecan-2 antibodies were relatively inefficient at immunoblotting (possibly due to the very heterogeneous size of syndecan-2 protein resulting

from glycosaminoglycan side chains); third, CASK almost certainly binds to multiple proteins via its PDZ domain (e.g., other syndecan family members and neuroligin), and hence only a fraction of CASK is likely to be complexed with syndecan-2 in the brain. In any case, the degree and significance of the CASK–syndecan interaction *in vivo* still needs to be confirmed by further biochemical and genetic experiments.

Discussion

Subcellular Distribution of CASK

Previous biochemical studies have shown that the CASK protein is enriched in the synaptic plasma membrane fraction of brain (Hata et al., 1996). Our subcellular fractionation extends this observation and reveals that CASK is

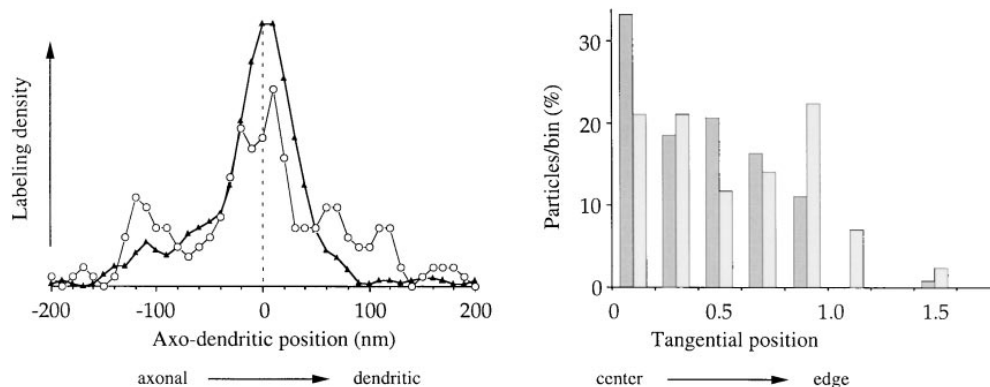


Figure 8. Quantitative analysis of syndecan and CASK immunogold EM. (*Left*) Graph compares axodendritic distribution of gold particles for syndecan-2 (filled triangles) and for CASK (open circles). Both antigens show the highest density at the synaptic junction (note that measurement error of immunogold labeling is $\sim \pm 20$ nm). CASK also exhibits smaller pre- and postsynaptic peaks. Although peaking at the syn-

aptic membrane, syndecan-2 labeling extends deeper into the presynaptic than the postsynaptic side. 0 (dotted line) represents outer leaflet of postsynaptic membrane. Data were collected from random fields from two animals, including 261 particles (for syndecan-2 labeling) and 63 particles (for CASK). To make the distribution pattern easier to see, data shown were digitally smoothed, using a three-point moving weighted average. (*Right*) Histogram compares tangential position of gold particles coding for syndecan-2 (shaded bars) and CASK (light bars). Only particles within 100 nm of the plasma membrane were considered. Tangential position for each gold particle with respect to the synaptic active zone (AZ) was normalized according to the following formula: $[(\text{distance to one end of AZ}) - (\text{distance to other end of AZ})] / (\text{total length of AZ})$. Thus, 0 corresponds to the AZ center, and 1 corresponds to the AZ edge. Both antigens were concentrated at the AZ, though more CASK was found at the periphery of the synapse and just outside it.

also enriched in the PSD fraction where it is at least partly resistant to detergent extraction. The synaptic localization of CASK, revealed for the first time by immunocytochemistry, is consistent with its interaction with syndecan-2 (an HSPG shown here to be concentrated in synapses) and with neuexins (which are believed to be at least partly synaptic in distribution; Hata et al., 1996). However, CASK is not exclusively localized in synapses; it is also present at nonsynaptic plasma membranes and in intracellular compartments. CASK may therefore be present at a variety of membrane domains in neurons, and its compartmentalization between membrane and cytoplasm may be dynamically regulated. Components of other cell junctional complexes have been shown to exist in both membrane-associated and cytoplasmic compartments, one example being β -catenin, which is both an adherens junction-associated and a cytoplasmic protein (reviewed in Miller and Moon, 1996).

Binding Specificity of the CASK PDZ Domain

The interacting clones captured by our two-hybrid screen suggest that the CASK PDZ domain has a binding selectivity for the COOH-terminal tetrapeptide consensus sequence -E-F-X-V/A (Table I). Neuexins, a family of transmembrane proteins previously shown to bind CASK (Hata et al., 1996), terminate in -EYYV, which conforms to this consensus. We show here that the neuexin COOH terminus also binds to CASK via the PDZ domain (Table I). The -E-F/Y-X-V/A consensus sequence, reached here on the basis of yeast two-hybrid assays, is consistent with that derived from peptide library screening using the CASK PDZ domain (Songyang et al., 1997). Both approaches reveal that the CASK PDZ domain selects for a valine or alanine at the COOH terminus (the 0 position) and an aromatic side chain residue (tyrosine or phenylalanine) at the -2 position. Thus, the CASK PDZ domain belongs to the class II PDZ domains, in contrast to the class I PDZ domains of the PSD-95 family of MAGUKs, which

prefer a serine or threonine at the -2 position (Songyang et al., 1997). These recognition specificities are in keeping with the fact that in *C. elegans* LIN-2 does not interact directly with LET-23/EGFR, which terminates with the sequence -ETCL.

We have shown that a tetrapeptide sequence (-EFYA, corresponding to the COOH-terminus of syndecan-2) is sufficient for specific interaction with the PDZ domain of CASK. By extrapolation, any protein that ends in the -E-F/Y-X-V/A consensus sequence may be capable of binding to CASK. Thus, the CASK PDZ domain may have multiple binding partners in vivo, just as the PDZs of PSD-95 can bind to several proteins with the COOH-terminal -E-S/T-X-V motif, including Shaker K^+ channels, NMDA receptors, and calcium pumps (Kim et al., 1998; Kim et al., 1995; Kornau et al., 1995; Niethammer et al., 1996). Consistent with the idea of multiple partners for CASK is that syndecan-2 distribution overlaps only partly with the distribution of CASK in neurons. Syndecan-2 is specifically localized in synaptic junctions, while CASK is more broadly distributed in synaptic and nonsynaptic sites and in intracellular compartments. Other potential ligands for CASK include the other members of the syndecan family, all four of which end in the identical COOH-terminal sequence of -EFYA (that we only isolated syndecan-2 in our two-hybrid screen may simply reflect the stochastic nature of the screening procedure). It is possible that other syndecans (particularly syndecan-3, which is relatively highly expressed in neurons) bind to CASK in nonsynaptic regions of the neuronal plasma membrane. In addition to the syndecans, of course, the neuexin intracellular COOH-terminal tail has specific affinity for the CASK PDZ (this study and Hata et al., 1996), and may be interacting with CASK in the brain. Neuexins are proposed to be at least in part present in synaptic membranes, based on their activity as latrotoxin receptors (Ushkaryov et al., 1992). The structure of neuexins, however, is extremely heterogeneous (Ullrich et al., 1995; Ushkaryov et al., 1992), and their subcellular distribution remains to be characterized in detail.

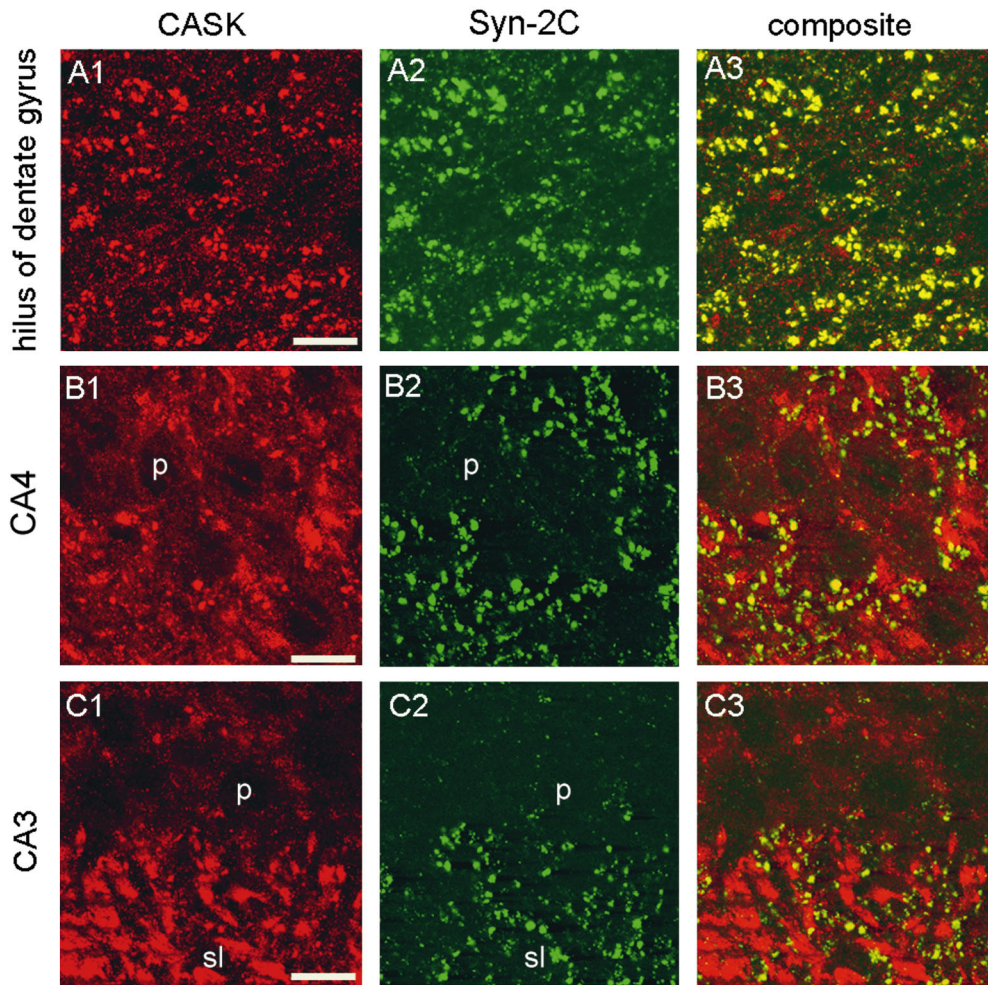


Figure 9. Partial colocalization of syndecan-2 and CASK in rat brain, shown by double label immunofluorescence confocal microscopy. (A) Hilar region of dentate gyrus; (B) CA4 (polymorphonuclear) region of hippocampus; (C) CA3 region. Each group of images ([A1–A3], [B1–B3], etc.) represents the same field visualized for CASK (Cy3/red) or for syndecan-2 (FITC/green), as indicated; composite images (A3, B3, and C3) show colocalization of CASK and syndecan-2 in yellow. P, pyramidal cells; sl, stratum lucidum. Bar, 20 μ m.

Possible Functions of the Syndecan–CASK Interaction

The syndecan family, consisting of four known members, constitutes a major form of heparan sulfate (HS) on the cell surface (reviewed in Bernfield et al., 1992; Carey, 1997; Couchman and Woods, 1996; David, 1993). Among the syndecans, conservation of sequence occurs only in their short intracellular COOH-terminal tails and in their transmembrane domains. Their striking sequence similarity had implied to many observers an important common function for intracellular COOH-terminal tails of syndecans. Here we show that one likely common function is to mediate binding to CASK, though the physiological significance of this interaction is still unknown.

Expression of syndecan HSPGs is regulated during development in a cell type–specific manner, and this regulation is believed to be important for dynamic cell–matrix interactions and for tissue morphogenesis (reviewed in Bernfield et al., 1992; Carey, 1997; Couchman and Woods, 1996; David, 1993). Transmembrane HSPGs such as syndecans may be involved in cell–matrix adhesion by binding to components of the extracellular matrix (ECM) including laminin, fibronectin, and collagen. By virtue of their interaction with CASK through their COOH-terminal tails, syndecans could provide a molecular bridge between the ECM and intracellular proteins. If CASK in turn interacts with cytoskeletal components such as protein 4.1 (Cohen

et al., cosubmitted manuscript), then a syndecan–CASK connection could link ECM to the intracellular cytoskeleton. In such a way, a syndecan–CASK interaction may contribute to adhesion of synaptic junctions, perhaps in conjunction with the known cadherin-based adhesion complex found at the periphery of synaptic active zones (reviewed in Serafini, 1997).

In addition to membrane proteins, MAGUK proteins can also interact with intracellular signaling molecules (such as nNOS, APC). By analogy with the integrin family of ECM receptors that nucleate an intracellular complex of proteins at the site of ECM contact (Clark and Brugge, 1995), the syndecan–CASK interaction might form the axis of a cytoskeletal/signaling complex at the plasma membrane. Since all syndecans terminate with the -EFYA sequence sufficient for binding to CASK, such a model may apply to other members of the family in addition to the synaptically localized syndecan-2.

Potential Significance of CASK–Syndecan Interaction in Growth Factor Signaling

Recently, interest has focused on cell surface HSPGs such as the syndecans because they bind to, and are essential for the biological actions of, certain secreted polypeptide factors (reviewed in Carey, 1997; Schlessinger et al., 1995). In the best-studied example of FGF signaling, cell surface

HSPGs are believed to be important for appropriate presentation of FGF to its high-affinity tyrosine kinase receptor, or for increasing the effective concentration of FGF at the plasma membrane. In this way, HSPGs at the plasma membrane can be regarded as coreceptors for heparin-binding factors, though of lower affinity and lower specificity than the specific receptor tyrosine kinases (reviewed in Carey, 1997; Schlessinger et al., 1995).

Bearing in mind that the CASK homolog LIN-2 is required for LET23/EGFR signaling in *C. elegans*, the question is raised: could the interaction between syndecan and CASK/LIN-2 play a role in growth factor signaling? We hypothesize that one function of CASK/LIN-2 is to bind and cluster syndecan HSPGs in the vicinity of the growth factor receptor. The HS side chains of syndecan can bind to many polypeptide growth/differentiation factors; this binding could enhance the action of the growth factor via a concentration effect or via appropriate presentation to its receptor tyrosine kinase. In the context of this model, it is noteworthy that the *C. elegans* syndecan protein also terminates in -EFYA, and is thus predicted to bind to LIN-2's PDZ domain. This prediction raises the possibility that loss-of-function of LIN-2 in *C. elegans* could inhibit LET23/EGF receptor signaling as a result of mislocalization of syndecan HSPGs. In vertebrates, HSPGs have been implicated in the action of neuregulin/ARIA, a heparin-binding secreted factor that acts on EGFR-like receptor tyrosine kinases (reviewed in Fischbach and Rosen, 1997). More intriguing is that neuregulin/ARIA is concentrated in the synaptic cleft of neuronal synapses (Sandrock et al., 1995), where it would be in a good position to interact with syndecan-2 HSPG. We speculate that synaptically localized syndecan HSPG may be involved in binding to certain growth factors (like neuregulins) in synapses, and in potentiating their action on synaptic receptor tyrosine kinases.

Previously, HSPGs have been localized in the vertebrate NMJ (Sanes, 1989; Sanes et al., 1986), but these HSPGs are either not identified or are thought to be associated with the ECM/basal lamina of the NMJ (e.g., agrin and perlecan). In this paper we find that brain synapses also contain a specific HSPG, thereby revealing a parallel with the NMJ; however, this HSPG is a transmembrane protein of the syndecan family rather than a predicted ECM protein. The localization of a cell surface HSPG in neuronal synapses sheds some new light on the molecular organization of synaptic junctions in the brain, and should provide a basis for further investigation into the molecules of the synaptic space.

The authors thank Dr. Merton Bernfield for the gift of MSE-2 syndecan-2 antibody, Drs. Graham Cowling and Thomas Südhof for providing syndecan-2 and CASK cDNA plasmids, Dr. James Anderson for helpful discussion and providing and hCASK plasmid and antibody, and Elaine Aidonis for help with the manuscript.

M. Sheng is an Assistant Investigator of the Howard Hughes Medical Institute. This work received support from National Institutes of Health Grant NS29879 (to R.J. Weinberg).

Received for publication 19 December 1997 and in revised form 13 May 1998.

References

Anderson, J.M. 1996. Cell signaling: MAGUK magic. *Curr. Biol.* 6:382-384.

- Bernfield, M., R. Kokenyesi, M. Kato, M.T. Hinkes, J. Spring, R.L. Gallo, and E.J. Lose. 1992. Biology of the syndecans: a family of transmembrane heparan sulfate proteoglycans. *Annu. Rev. Cell Biol.* 8:365-393.
- Brennan, J.E., D.S. Chao, S.H. Gee, A.W. McGee, S.E. Craven, D.R. Santillano, Z. Wu, F. Huang, H. Xia, M.F. Peters, et al. 1996. Interaction of nitric oxide synthase with the postsynaptic density protein PSD-95 and α 1-syntrophin mediated by PDZ domains. *Cell* 84:757-767.
- Carey, D. 1997. Syndecans: multifunctional cell-surface co-receptors. *Biochem. J.* 327:1-16.
- Cho, K.-O., C.A. Hunt, and M.B. Kennedy. 1992. The rat brain postsynaptic density fraction contains a homolog of the drosophila discs-large tumor suppressor protein. *Neuron* 9:929-942.
- Clark, E.A., and J.S. Brugge. 1995. Integrins and signal transduction pathways: the road taken. *Science* 268:233-239.
- Couchman, J.R., and A. Woods. 1996. Syndecans, signaling, and cell adhesion. *J. Cell Biochem.* 61:578-584.
- David, G. 1993. Integral membrane heparan sulfate proteoglycans. *FASEB J.* 7:1023-1030.
- Dimitratos, S.D., D.F. Woods, and P.J. Bryant. 1997. Camguk, lin-2 and CASK: novel membrane-associated guanylate kinase homologs that also contain CaM kinase domains. *Mech. Dev.* 63:127-130.
- Fischbach, G.D., and K.M. Rosen. 1997. ARIA: A neuromuscular junction neu-regulin. *Annu. Rev. Neurosci.* 20:429-458.
- Hata, Y., S. Butz, and T.C. Südhof. 1996. CASK: a novel *dlg*/PSD95 homolog with an N-terminal calmodulin-dependent protein kinase domain identified by interaction with neurexins. *J. Neurosci.* 16:2488-2494.
- Hoskins, R., A.F. Hajnal, S.A. Harp, and S.K. Kim. 1996. The *C. elegans* vulval induction gene *lin-2* encodes a member of the MAGUK family of cell junction proteins. *Development* 122:97-111.
- Hsueh, Y.-P., E. Kim, and M. Sheng. 1997. Disulfide-linked head-to-head multimerization in the mechanism of ion channel clustering by PSD-95. *Neuron* 18:803-814.
- Kim, C.W., O.A. Goldberger, R.L. Gallo, and M. Bernfield. 1994. Members of the syndecan family of heparan sulfate proteoglycans are expressed in distinct cell-, tissue-, and development-specific patterns. *Mol. Biol. Cell* 5:797-805.
- Kim, E., K.-O. Cho, A. Rothschild, and M. Sheng. 1996. Heteromultimerization and NMDA receptor-clustering activity of chapsyn-110, a member of the PSD-95 family of proteins. *Neuron* 17:103-113.
- Kim, E., S.T. DeMacro, S.M. Marfatia, A.H. Chishti, M. Sheng, and E.E. Strehler. 1998. Plasma membrane Ca^{2+} ATPase isoform 4b binds to membrane-associated guanylate kinase (MAGUK) proteins via their PDZ domains. *J. Biol. Chem.* 273:1591-1595.
- Kim, E., S. Naisbitt, Y.-P. Hsueh, A. Rao, A. Rothschild, A.M. Craig, and M. Sheng. 1997. GKAP, a novel synaptic protein that interacts with the guanylate kinase-like domain of the PSD-95/SAP90 family of channel clustering molecules. *J. Cell Biol.* 136:669-678.
- Kim, E., M. Niethammer, A. Rothschild, Y.N. Jan, and M. Sheng. 1995. Clustering of shaker-type K^{+} channels by interaction with a family of membrane-associated guanylate kinases. *Nature* 378:85-88.
- Kim, S.K. 1995. Tight junctions, membrane-associated guanylate kinases and cell signaling. *Curr. Opin. Cell Biol.* 7:641-649.
- Kornau, P., P. Seeburg, and M. Kennedy. 1997. Interaction of ion channels and receptors with PDZ domain proteins. *Curr. Opin. Neurobiol.* 7:368-373.
- Kornau, H.-C., L.T. Schenker, M.B. Kennedy, and P.H. Seeburg. 1995. Domain interaction between NMDA receptor subunits and the postsynaptic density protein PSD-95. *Science* 269:1737-1740.
- Lue, R.A., E. Brandin, E.P. Chan, and D. Branton. 1996. Two independent domains of hDlg are sufficient for subcellular targeting: the PDZ1-2 conformational unit and an alternatively spliced domain. *J. Cell Biol.* 135:1125-1137.
- Marfatia, S.M., J.H.M. Cabral, L. Lin, C. Hough, P.J. Bryant, L. Stolz, and A.H. Chishti. 1996. Modular organization of the PDZ domains in the human discs-large protein suggests a mechanism for coupling PDZ domain-binding proteins to ATP and the membrane cytoskeleton. *J. Cell Biol.* 135:753-766.
- Matsumine, A., A. Ogai, T. Senda, N. Okumura, K. Satoh, G.-H. Baeg, T. Kawahara, S. Kobayashi, M. Okada, K. Toyoshima, and T. Akiyama. 1996. Binding of APC to the human homolog of the *Drosophila* discs large tumor suppressor protein. *Science* 272:1020-1023.
- Miller, J.R., and R.T. Moon. 1996. Signal transduction through β -catenin and specification of cell fate during embryogenesis. *Genes Dev.* 10:2527-2539.
- Müller, B.M., U. Kistner, R.W. Veh, C. Cases-Langhoff, B. Becker, E.D. Gundelfinger, and C.C. Garner. 1995. Molecular characterization and spatial distribution of SAP97, a novel presynaptic protein homologous to SAP90 and the *Drosophila* discs-large tumor suppressor protein. *J. Neurosci.* 15:2354-2366.
- Naisbitt, S., E. Kim, R.J. Weinberg, A. Rao, F.-C. Yang, A.M. Craig, and M. Sheng. 1997. Characterization of guanylate kinase-associated protein, a postsynaptic density protein at excitatory synapses that interacts directly with postsynaptic density-95/synapse-associated protein 90. *J. Neurosci.* 17:5687-5696.
- Niethammer, M., E. Kim, and M. Sheng. 1996. Interaction between the C terminus of NMDA receptor subunits and multiple members of the PSD-95 family of membrane-associated guanylate kinases. *J. Neurosci.* 16:2157-2163.
- Phend, K.D., R.J. Weinberg, and A. Rustioni. 1992. Techniques to optimize post-embedding single and double staining for amino acid neurotransmitters. *J. Histochem. Cytochem.* 40:1011-1020.
- Phend, K.D., A. Rustioni, and R.J. Weinberg. 1995. An osmium-free method of

- Epon embedment that preserves both ultrastructure and antigenicity for postembedding immunocytochemistry. *J. Histochem. Cytochem.* 43:283–292.
- Sandrock, J., W. Alfred, A.D.J. Goodearl, Q.-W. Yin, D. Chang, and G.D. Fischbach. 1995. ARIA is concentrated in nerve terminals at neuromuscular junctions and at other synapses. *J. Neurosci.* 15:6124–6136.
- Sanes, J.R. 1989. Extracellular matrix molecules that influence neural development. *Annu. Rev. Neurosci.* 12:491–516.
- Sanes, J.R., M. Schachner, and J. Covault. 1986. Expression of several adhesive macromolecules (N-CAM, L1, J1, NILE, uvomorulin, laminin, fibronectin, and a heparan sulfate proteoglycan) in embryonic, adult, and denervated adult skeletal muscle. *J. Cell Biol.* 102:420–431.
- Serafini, T. 1997. An old friend in a new home: cadherins at the synapse. *Trends Neurosci.* 20:322–323.
- Satoh, K., H. Yanai, T. Senda, K. Kohu, T. Nakamura, N. Okumura, A. Matsumine, S. Kobayashi, K. Toyoshima, and T. Akiyama. 1997. DAP-1, a novel protein that interacts with the guanylate kinase-like domains of hDLG and PSD-95. *Genes Cells.* 2:415–424.
- Schlessinger, J., I. Lax, and M. Lemmon. 1995. Regulation of growth factor activation by proteoglycans: what is the role of the low affinity receptors? *Cell.* 83:357–360.
- Sheng, M. 1996. PDZs and receptor/channel clustering: rounding up the latest suspects. *Neuron.* 17:575–578.
- Sheng, M., and E. Kim. 1996. Ion channel associated proteins. *Curr. Opin. Neurobiol.* 6:602–608.
- Sheng, M., J.Y. Liao, Y.N. Jan, and L.Y. Jan. 1993. Presynaptic A-current based on heteromultimeric K⁺ channels detected in vivo. *Nature.* 365:72–75.
- Sheng, M., M.-L. Tsaur, Y.N. Jan, and L.Y. Jan. 1994. Contrasting subcellular localization of the Kv1.2 K⁺ channel subunit in different neurons of rat brain. *J. Neurosci.* 14:2408–2417.
- Shindler, K.S., and K.A. Roth. 1996. Double immunofluorescent staining using two unconjugated primary antisera raised in the same species. *J. Histochem. Cytochem.* 44:1331–1335.
- Simske, J.S., S.M. Kaech, S.A. Harp, and S.K. Kim. 1996. LET-23 receptor localization by the cell junction protein LIN-7 during *C. elegans* vulval induction. *Cell.* 85:195–204.
- Songyang, Z., A.S. Fanning, C. Fu, J. Xu, S.M. Marfatia, A.H. Chishti, A. Crompton, A.C. Chan, J.M. Anderson, and L.C. Cantley. 1997. Recognition of unique carboxyl-terminal motifs by distinct PDZ domains. *Science.* 275:73–77.
- Takeuchi, M., Y. Hata, K. Hirao, A. Toyoda, M. Irie, and Y. Takai. 1997. SAPAPs, a family of PSD-95/SAP90-associated proteins localized at postsynaptic density. *J. Biol. Chem.* 272:11943–11951.
- Ullrich, B., Y.A. Ushkaryov, and T.C. Südhof. 1995. Cartography of neurexins: more than 1000 isoforms generated by alternative splicing and expressed in distinct subsets of neurons. *Neuron.* 14:497–507.
- Ushkaryov, Y.A., A.G. Petrenko, M. Geppert, and T.C. Südhof. 1992. Neurexins: synaptic cell surface proteins related to the α -latrotoxin receptor and laminin. *Science.* 257:50–56.